processes

Article

Topology-Based Initialization for the Optimization-Based Design of Heteroazeotropic Distillation Processes

Kai Fabian Kruber * and Mirko Skiborowski

Institute of Process Systems Engineering, Hamburg University of Technology, Am Schwarzenberg-Campus 4, D-21073 Hamburg, Germany; mirko.skiborowski@tuhh.de
* Correspondence: kai.kruber@tuhh.de; Tel.: +49-40-42878-3148

Abstract: Distillation-based separation processes, such as extractive or heteroazeotropic distillation, present important processes for separating azeotropic mixtures in the chemical and biochemical industry. However, heteroazeotropic distillation has received much less attention than extractive distillation, which can be attributed to multiple reasons. The phase equilibrium calculations require a correct evaluation of phase stability, while the topology of the heterogeneous mixtures is generally more complex, comprising multiple azeotropes and distillation regions, resulting in an increased modeling complexity. Due to the integration of distillation columns and a decanter, even the simulation of these processes is considered more challenging, while an optimal process design should include the selection of a suitable solvent, considering the performance of the integrated hybrid process. Yet, the intricate mixture topologies largely impede the use of simplified criteria for solvent selection. To overcome these limitations and allow for a process-based screening of potential solvents, the current work presents a topology-based initialization and optimization approach for designing heteroazeotropic distillation processes. The systematic initialization enables an efficient evaluation of different solvents with different mixture topologies, which is further exploited for optimization-based sensitivity analysis and multi-objective optimization. Three case studies are analyzed with about 170 individually optimized process designs, including stage numbers, feed locations, phase ratios, and heat duties.

Keywords: heteroazeotropic distillation; process design; optimization; solvent screening; sensitivity analysis; multi-objective optimization

Citation: Kruber, K.F.; Skiborowski, M. Topology-Based Initialization for the Optimization-Based Design of Heteroazeotropic Distillation Processes. *Processes* **2022**, *10*, 1482. https://doi.org/10.3390/pr10081482

Academic Editor: Blaž Likozar

Received: 5 July 2022
Accepted: 26 July 2022
Published: 28 July 2022

1. Introduction

Separating azeotropic mixtures is a critical challenge in the downstream processing for the production of bulk and specialty chemicals in the chemical and biochemical industry. Besides the widely applied and well-investigated extractive distillation [1], heteroazeotropic distillation is another proven technology to effectively separate these kinds of mixtures in medium to large-scale processes [2]. In heteroazeotropic distillation processes, either the partial immiscibility of a given mixture is exploited or an additional solvent is applied, inducing partial immiscibility to overcome the limitation of an azeotrope or distillation boundary [3]. Like extractive distillation processes, heteroazeotropic distillation processes consist of two interconnected distillation columns, which both purify one of the desired products. An integrated decanter performs a separation of two immiscible liquid phases at potentially sub-cooled conditions to overcome the inherent distillation boundaries. The existence of a heterogeneous azeotrope is a general prerequisite for the feasibility of the process. Since heteroazeotropes are always minimum boiling azeotropes [4], the azeotrope can either be characterized as a saddle or an unstable node in respect of the mixture topology [5]. This is explained by Kiva et al. [4] based on physical reasoning, concluding that heterogeneity (liquid-liquid phase splitting) and minimum-boiling azeotropes occur

when the different components of the mixture repel each other. In contrast, maximum-boiling azeotropes occur when the components attract each other.

Yet, the sole existence of a heteroazeotrope does not allow for an evaluation of the suitability of a heteroazeotropic distillation process. The identification of suitable solvents for heteroazeotropic distillation is either based on heuristic guidelines [6] or the use of computer-aided molecular design (CAMD) methods [7]. However, both of these methods require subsequent confirmation of the feasibility considering the multi-component multi-phase interactions, either using a proper process simulation or graphical analysis of the mixture topology [8]. Kiva et al. [4] describe several topologies for ternary mixtures that are considered suitable candidates for heterogeneous azeotropic distillation. These complex topologies have a miscibility gap with several azeotropes, resulting in multiple distillation regions and highlighting the highly non-ideal phase behavior. The intricacy inhibits the use of simple process performance indicators for the selection of solvents, such as distribution coefficients and selectivities at infinite dilution in liquid-liquid extraction or adjusted relative volatilities in extractive distillation [9,10].

Similarly, the use of simulation models is challenging, as stated by Luyben [11], who simulated a heteroazeotropic distillation process in the commercial flowsheet simulator Aspen Plus® for the dehydration of ethanol with a particular focus on the manual initialization procedure. To initialize the heteroazeotropic column, they started by estimating the compositions and flow rates of the organic reflux and the recycle stream of the second column. They reported that the simulation of this single column is already "extremely tricky" since multiple steady states are present and the product compositions are susceptible to changes in the organic reflux [11]. Subsequently, they added the second column and adjusted the degrees of freedom to match the purity specifications for both product streams. Although a profound and detailed initialization strategy was used, they concluded with a non-converged simulation. The presence of multiple steady states induced by the highly non-ideal phase behavior makes the manual adjustment of the degrees of freedom a demanding task. Even if an initial feasible flowsheet simulation is available, further process optimization can be tedious, as confirmed by Huang et al. [12], who optimized an industrial process for the dehydration of acetic acid, building on a previously developed simulation model that was validated by real-world results of an industrial plant. Despite the existence of the simulation model, Huang et al. [12] report a considerable effort for the manual adaptation of the operation of the individual units. Consequently, there is a significant potential for optimization-based design methods, which allow for simultaneous optimization of all design degrees of freedom.

The combination of a metaheuristic and a commercial flowsheet simulator is a widely applied approach for optimizing distillation-based separation processes [13–15]. However, this combination usually requires the availability of a feasible initial solution, which maintains the previously described challenges of manual initialization. Consequently, the application to heteroazeotropic distillation is scarce, with the only reported approach by Ramanathan et al. [16]. The authors assume constant molar overflow and no phase splitting in the entire column, limiting the phase equilibrium calculations to vapor-liquid-equilibrium (VLE) calculations. However, the correct identification of three-phase vapor-liquid-liquid equilibrium (VLLE) solutions is of vital importance and ignoring the second liquid phase may result in substantial calculation errors [17,18]. In contrast to a metaheuristic approach, Franke [19] used a generalized benders decomposition algorithm to determine the optimal design of a heteroazeotropic distillation process for ethanol dehydration based on a simulation model in Aspen Plus. Franke [19] highlights the importance of a robust simulation model while applying dedicated flash calculations subsequent to the individual simulation runs to evaluate the phase stability on every tray. The particular post-processing procedure with potential re-initialization is applied to overcome numerical problems, which are not expected to appear in problems in real applications [20]. Although Franke [19] describes the necessity of an initial feasible converged simulation as no limitation, assuming that sim-

ulation studies always precede process optimization in practice, the limitations described by Luyben [11] remain a major challenge.

Overall, there has been considerably less focus on heteroazeotropic distillation than extractive distillation. Skiborowski et al. [18] provide a detailed overview of the methodological work regarding the design of heteroazeotropic distillation processes, covering entrainer selection, analysis of the mixture topology, and the design problem, as well as both shortcut and rigorous design methods up until 2015. The subsequent period from 2015–2021 is covered in the recent review article of Yang Kong et al. [21], who provide a more general overview of recent process design studies for the separation of azeotropic mixtures. Besides confirming the prevalence of studies on extractive distillation, the review further reveals an increasing trend towards research focusing on energy efficiency and heat integration. The complexity of the phase equilibrium modeling and the process configurations are likely one of the primary reasons that these configurations are less studied compared to pressure-swing and extractive distillation processes. One of the few reported studies on heteroazeotropic distillation covers the optimization of different heteroazeotropic and pressure-swing distillation processes separating isopropanol, diisopropyl ether, and water in a series of papers by [22–24]. Considering the basic processes, including heat integration for pressure-swing distillation in a comparative study [22] , as well as hybrid versions of both processes, including intensified process variants, like dividing wall columns [23,24], the authors, applied a sequential iterative optimization procedure for the optimization of the total annualized costs (TAC) as the objective function. Considering the given mixtures' complexity, the reported results are impressive and illustrate the benefits of heteroazeotropic distillation and potential means for energy integration. Yet, the approach still builds on the use of a flowsheet simulator, maintaining the previously described limitations.

To overcome several of these limitations, Skiborowski et al. [18] proposed an optimization-based approach for the conceptual design of heteroazeotropic distillation processes, which effectively integrates a numerically efficient and robust phase stability test [25] that is introduced in an equation-oriented mixed-integer nonlinear programming (MINLP) problem via external functions. This nested model formulation allows for the correct consideration of VLE or VLLE solutions for each of the present equilibrium trays, while a sequential initialization procedure based on a polylithic solution approach is supposed to overcome the need for an initial feasible solution. The successful application of the optimization-based approach was demonstrated for several flowsheet configurations and different separation problems, including the dehydration of 1-hexanol, isopropanol, an n-butyl acetate/n-butanol/acetic acid mixture, and a 2-methyltetrahydrofuran/1-pentanol mixture. The proposed modeling and solution procedure either starts with a simple initial flash calculation for the feed stream to initialize a simple column model, which is further transformed into a hybrid configuration of a heteroazeotropic distillation column with a decanter, or it builds on provisional results from preceding shortcut computations, for which the feed angle method is applied [26]. The latter is essential for complex configurations, such as the isopropanol dehydration case study. With proper initialization, the optimization-based approach provides further potential for screening alternative solvents or process configurations and means for energy integration. The latter was demonstrated recently by Waltermann et al. [27], who highlight the possible application for benchmarking extractive and heteroazeotropic distillation for the dehydration of ethanol considering direct heat integration, vapor recompression, and thermal coupling in a dividing wall column as additional means for process intensification. The evaluation of different solvents was also considered by Waltermann et al. [27] for extractive distillation, while the more complex and variable topology of heteroazeotropic mixtures presents an additional challenge for a direct transfer to heteroazeotropic distillation processes.

This issue is addressed in the current publication by means of a topology-based initialization, which effectively overcomes the need for preceding shortcut calculations. The novel initialization procedure allows for a direct consideration of simple and heteroazeotropic columns in the polylithic modeling and solution approach, improving the robustness and enabling the consideration of different mixture topologies for alternative solvents. Thus,

the approach extends the range of potential applications of the optimization-based design approach to an efficient solvent screening and allows for an integration of multi-objective optimization and parallelized sensitivity analyses, building on locally optimized process configurations.

For clarity, Section 2 first briefly describes the superstructure formulation for the considered heteroazeotropic distillation process, the respective equilibrium-stage model, and the specification of the MINLP problem with sizing and cost estimation. The topology-based initialization procedure is further described in detail for the three most common topologies of ternary mixtures for solvent-based heteroazeotropic distillation [4]. The application of the approach is illustrated in Section 3 for three respective case studies as real representative systems for the considered topologies, investigating the dehydration of ethanol with different solvents, the separation of ethyl acetate and isooctane with acetonitrile as solvent, and the dehydration of 1,4-dioxane using benzene. Finally, Section 4 provides a conclusion and indicates potential applications and future work.

2. Methodology

The conceptual design of the heteroazeotropic distillation process is posed as an MINLP problem, which is solved as a series of successively relaxed MINLP (SR-MINLP) problems following the strategy proposed by Kraemer et al. [28] and further refined for heteroazeotropic distillation processes by Skiborowski et al. [18]. The final optimization problem consists of an economic objective function related to the TAC, which are determined based on a superstructure model for the process and additional sizing and costing correlations introduced as equality constraints. Unlike a simulation-based design procedure, the presented approach automatically determines the main design parameters of the individual flowsheet such that the desired product purities are obtained and the economic objective function is minimized. The following subsections first provide a summary of the superstructure model and the sizing and costing correlations, while the novel topology-based initialization and solution approach is outlined in Section 2.2 before the specific approach for the sensitivity analysis and multi-objective optimization is presented.

2.1. Superstructure Model

The conceptual superstructure model of the heteroazeotropic distillation process considered in the current work is illustrated in Figure 1. The process consists of a combination of a simple distillation column and a subsequent heteroazeotropic distillation column with the decanter integrated into the reflux and the recycle of the top product of the heteroazeotropic column to the simple column. Accordingly, both product streams are obtained as the bottom product of the individual columns. The superstructure model is solved in an equation-oriented manner and allows for a variable position of the reflux and boil-up streams, resulting in an effective bypass of the equilibrium trays above the reflux location and below the boil-up location. Thus, the number of equilibrium trays and the feed location are degrees of freedom in the optimization. The superstructure model is formulated in GAMS with the aforementioned external functions provided as a direct link library.

The individual column stages are modeled as equilibrium trays based on the common MESH model, considering mass balances, equilibrium conditions, summation constraints, and enthalpy balances. In case of bypassing the boil-up or reflux stream, either the entering vapor or liquid stream is zero for the individual stage. However, this does not cause any problem, assuming that a saturated vapor or liquid stream will leave the stage unchanged in accordance with the maintained phase equilibrium. As previously stated, the equilibrium computations are performed by means of external functions that integrate the numerically efficient and robust phase stability test proposed by Bausa and Marquardt [25] to evaluate the correct phase equilibrium solution. In the case of a three-phase VLLE solution, a corresponding (quasi) VLE solution is determined, including the computation of the specific enthalpy of the liquid phase. Thus, the column model considers only the overall liquid composition, while the individual

phase compositions and phase ratio for a VLLE solution are only handled in the external function. This reformulation effectively avoids discontinuities resulting from the transition between homogeneous and heterogeneous phase equilibria and enables a gradient-based optimization. Refer to the preceding article of Skiborowski et al. [18] for further details on the phase equilibrium computations and the external functions. The latter are available as open source code within the process synthesis software collection provided under a General Public License by RWTH Aachen University [29].

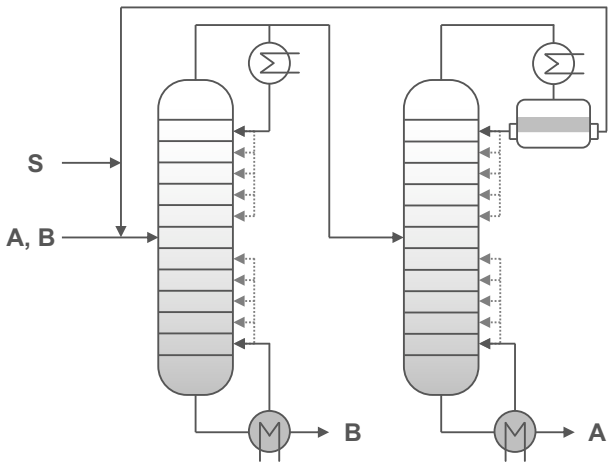

Figure 1. Superstructure for the optimization of a heteroazeotropic distillation process.

To evaluate the economic objective function in terms of the TAC, the superstructure model is augmented with additional equations for equipment sizing accounting for the column shell, internals, and heat exchangers [28,30] as well as respective cost correlations for the individual equipment [31,32]. The estimated investment costs are updated with the CEPCI index of September 2017 [33] and the respective capital expenditures (CAPEX) are calculated by the total investment costs and a depreciation time of ten years with an interest rate of 6%. The operational expenditures (OPEX) account for the necessary utility streams and the makeup stream for potential solvent loss. The columns are operated at atmospheric pressure for all case studies considered in Section 3. The respective utility costs are assumed as 12 € $\cdot$ t^{-1} for 3 bar steam and 0.05 € $\cdot$ t^{-1} for cooling water. An operating time of 8000 h $\cdot$ a^{-1} is assumed. The equipment costs for the decanter are not considered since a reliable size estimate requires knowledge of the disengagement time, which is considered unknown during early the conceptual design phase [18].

The resulting MINLP problem is highly nonlinear, primarily because of the respective thermodynamic models required to accurately describe the complex VLE/VLLE relationships. In order to enable a numerically efficient and robust local optimization, the binary variables for the location of the reflux and boil-up streams are initially relaxed and subsequently tightened by solving a series of nonlinear programming (NLP) problems with additional nonlinear complementary constraints (NCP) [28]. Here, the NCP-functions are introduced as penalty terms for the objective to force the continuous decision variables for reflux and reboil stages to integer values by gradually increasing the penalty weighting. However, the complex mixture topologies with multiple azeotropes and distillation regions mandate a proper initialization to successfully solve the final SR-MINLP problem. Therefore, another key feature introduced in the current contribution is the topology-based initialization approach described in the subsequent section.

2.2. Topology-Based Initialization and Solution Strategy

While the phase equilibrium information of chemical systems can be more or less complex, the information about the number and type of singular points allows for a characterization of the individual mixture and the analysis of viable products, distillation regions, and potentially even process synthesis [5,34,35]. Due to the potential graphical

analysis of residue curve maps and distillation line maps, especially ternary mixtures have been heavily investigated. Kiva et al. [4] and Kiva and Krolikowski [36] provide detailed analysis of ternary mixtures and the suitability of azeotropic distillation processes for separating certain mixture topologies. For the application of heteroazeotropic distillation, the general topology of a ternary mixture is composed of the azeotropic binary subsystem, which is to be separated using the additional solvent that introduces a minimum-boiling heterogeneous azeotrope. Kiva et al. [4] indicate that primarily three topologies cover the majority of real mixtures. These topologies are illustrated in Figure 2.

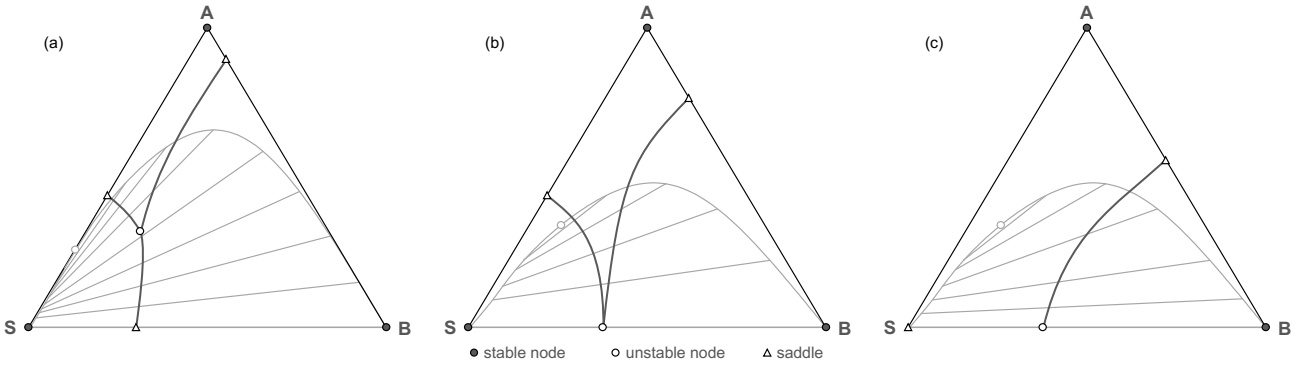

Figure 2. Depiction of the three ternary topologies that are most common when dealing with heteroazeotropic distillation, comprising four (**a**), three (**b**), and two (**c**) azeotropes.

Obviously, all topologies exhibit a miscibility gap, a binary homogeneous, and a heterogeneous azeotrope. They do, however, vary in the number of binary azeotropes and the existence of a ternary heteroazeotrope:

- Topology (a) indicates additionally a heterogeneous ternary azeotrope as well as another binary homogeneous azeotrope. Generally, the ternary azeotrope is the unstable node of the system, while all binary azeotropes are saddles. As a result, there are three distillation regions and six compartments, which makes topology (a) particularly complex. According to Kiva et al. [4] and their personal correspondence with Reshetov, this topology is the most frequent and occurred in 26% of the investigated 1365 azeotropic mixtures between 1965 and 1988.
- Topology (b) exhibits an additional binary homogeneous azeotrope. The heterogeneous binary azeotrope is the unstable node of the system, while the two homogeneous azeotropes are saddles resulting in three distillation regions but only four compartments. This mixture occurred in 8.4% of the cases reported within the survey of Kiva et al. [4].
- Topology (c) introduces no new azeotropes and is the simplest of the three topologies. With the heteroazeotrope as an unstable node and the homogeneous azeotrope as a saddle, the mixture has two distillation regions with two compartments in the region containing the solvent. According to Kiva et al. [4], the occurrence of this topology is about 21% with respect to the investigated mixtures by Reshetov.

Despite the complexity, these topologies are listed among the most common ternary mixtures. The remaining topologies, which are not considered in the current study, exhibit only a single azeotrope. In consequence, these systems are not representative of a solvent-based separation. Skouras and Skogestad [37] consider such systems in a study that focuses on ternary heteroazeotropic batch distillation investigating the separation of self-entrained systems. The authors provide a general guideline for the feasibility of separating ternary heteroazeotropic mixtures in a batch multivessel-decanter hybrid setup.

As outlined in previous publications for shortcut-based screening [26,38,39], the knowledge of the topology and the locations of the singular points indicate the composition profiles that can be obtained in distillation columns at total reflux. The current work proposes a direct utilization of this knowledge for an improved initialization procedure, which

follows the subsequent sequence of steps, which are further outlined in Figure 3 for the most common topology (cf. Figure 2a):

(1) Calculation and characterization of all azeotropes, e.g., based on the continuation approach proposed by Fidkowski et al. [40] or the unifying approach proposed by Skiborowski et al. [5] (cf. Figure 3a).
(2) Determination of the two liquid phase compositions resulting from the phase separation of the heterogeneous azeotrope with the lowest boiling point (cf. Figure 3b).
(3) Setting up and solving a mass-balance-based model of the integrated overall process assuming that both columns produce pure product streams of components A and B, respectively. Furthermore, the top vapor stream in the heterogeneous column is assumed to have the composition of the low boiling heterogeneous azeotrope regardless of whether it is a ternary (topology (a)) or a binary azeotrope (topology (b) or (c)). The decanter completely separates the two phases and the solvent-lean phase is considered as distillate product, which is recycled to the simple distillation column. As an objective function, the fresh solvent stream is minimized by varying the amount of the product streams as well as the composition of the product stream of the homogeneous distillation column. This step is similar to the application of the ∞/∞-approach described by Ryll et al. [38] and provides estimates for the top product compositions and the recycle stream (cf. Figure 3c).
(4) Next, the initialization of the simple column is performed based on the estimate of the mixed feed stream containing the fresh feed and the process recycle (cf. Figure 3d). The initialization and solution comprise a polylithic modeling approach, beginning with the individual flash calculation of the mixed feed stream and subsequent solution of the MESH model with a fixed structure, followed by a minimization of the heat duty.
(5) The initialization of the heterogeneous column builds on an initial column profile approximated by a piecewise linear connection of the minimum-boiling heterogeneous azeotrope, the desired product (component A), and the intermediate saddle(s) in the respective distillation region. For topology (a) in Figure 3e, the profile is composed of the upper part of the binary edge between component A and solvent S as well as the direct connection between the AS azeotrope and the ternary heteroazeotrope. For topology (b), the saddle is the homogeneous azeotrope between component A and solvent S, which is further connected to the binary heteroazeotrope between component B and solvent S. For topology (c), the saddle is the pure solvent S, such that the column profile is approximated by the binary edge between A and S as well as the part of the binary edge between solvent S and the heteroazeotrope. Based on the initial profile, the individual phase equilibrium on each stage is evaluated before the full column model is solved. Finally, the heat duty is minimized, considering that the model can feed a mixture of both phases from the decanter as a reflux stream to the column and can withdraw a mixed stream as a recycle to the simple column (cf. Figure 3f).
(6) Finally, the individual column models are joined to evaluate the minimum heat required for the separation given the maximum number of available equilibrium trays prior to the optimization of the superstructure.

The described initialization procedure integrates the knowledge of the mixture topology for an initial estimate of the unknown product compositions as well as the internal composition profile for the heteroazeotropic distillation column. Furthermore, the individual complexity of the models is gradually increased in the polylithic modeling and solution approach. As a final step, sizing and cost correlations are introduced and the TAC are determined for a fixed process structure and subsequently optimized for a free superstructure based on the SR-MINLP problems.

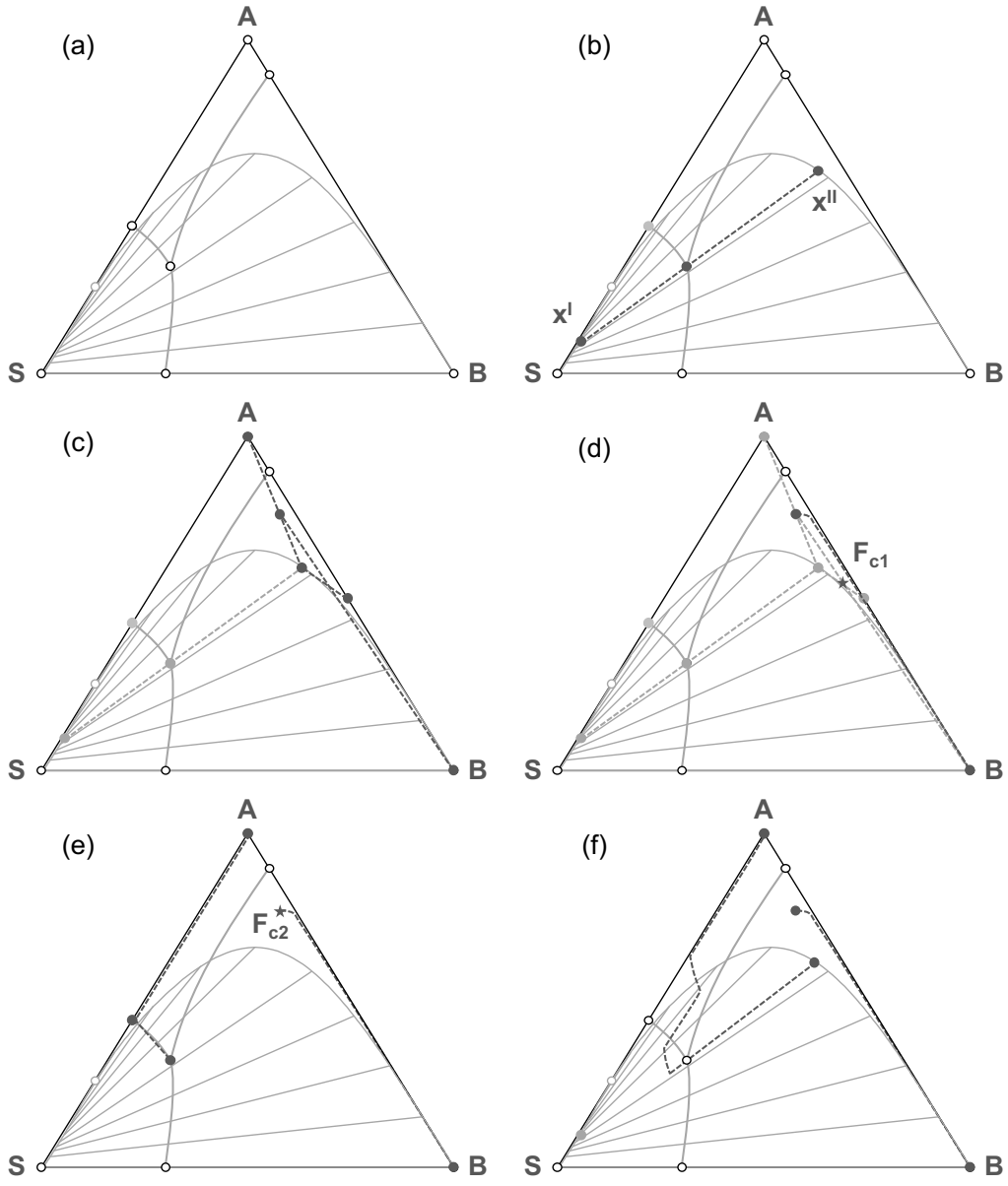

Figure 3. Depiction of the initialization procedure for heteroazeotropic distillation columns exemplarily demonstrated for a ternary minimum-boiling azeotrope. (**a**) Determination of azeotropes, (**b**) decanter calculation, (**c**) solving overall mass balances, (**d**) calculation of the homogeneous column, (**e**) initial composition profile of the heteroazeotropic column, (**f**) calculation of the heteroazeotropic column.

2.3. Automatic Sensitivity Studies and Multi-Objective Optimization

The topology-based initialization and the subsequent superstructure optimization overcome the need for an initially feasible process simulation to derive an optimized process design. This enables several interesting applications, one of which is the screening of alternative solvents. However, further applications include the evaluation of uncertain parameters by means of sensitivity studies or the consideration of multiple competing objectives. Sensitivity studies may, e.g., be performed with respect to uncertain property data or variations in product or feed specifications. Based on the proposed approach, a locally optimized process design can be determined for each scenario by a simple variation of the initial parametrization.

Considering multiple objective functions complicates the optimization since a set of effective or Pareto-optimal solutions needs to be determined [41]. The consideration of multiple objectives can be addressed in various ways. The most common strategies are the weighted-sum approach [42,43], the ϵ-constraint method [44], the normal boundary method [45], and genetic algorithms [46,47]. As most of these methods build on the efficient solution of a series of modified single-objective optimization (SOO) problems, the proposed initialization and optimization approach can be utilized effectively. In this work, a simple weighted-sum approach with normalized objectives [48,49] is used to generate a set of Pareto-optimal solutions. This approach was previously illustrated for optimizing a dividing wall column by Waltermann and Skiborowski [50], considering the minimization of CAPEX and OPEX as individual and competing objectives. The multi-objective optimization (MOO) problem is therefore solved as a series of SOO problems with the objective function *obj* as a weighted sum of the normalized values:

$$obj = w\frac{\text{CAPEX}}{\text{CAPEX}_{\text{nadir}}} + (1-w)\frac{\text{OPEX}}{\text{OPEX}_{\text{nadir}}}. \quad (1)$$

Here, the reference values, $\text{CAPEX}_{\text{nadir}}$ and $\text{OPEX}_{\text{nadir}}$, are the corresponding objective values for an a-priori calculated Nadir point [51], which is obtained by optimizations w.r.t. only one of the objective functions at a time. One key challenge for the weighted-sum method is the identification of proper weights. There are multiple methods to effectively assign weights to calculate an approximation of the Pareto front, like the extended sandwich method by Burger et al. [52], while reducing the number of necessary function evaluations. However, a simple equidistant weight distribution is sufficient for the current application to approximate the Pareto front.

3. Results

In order to illustrate the applicability and highlight the advantages of the proposed approach, three case studies are evaluated. The specific mixtures represent real applications and cover the most common three ternary mixture topologies illustrated in Figure 2. The calculations are performed using GAMS 24.9.2 (General Algebraic Modeling System) with the sequential quadratic programming solver SNOPT for the solution of the individual NLP problems on a computer with an Intel® Xeon™ Gold 5118 CPU with 24 cores (2.30 GHz) and 96 GB RAM.

3.1. Ethanol Dehydration

The first case study considers the dehydration of ethanol, an essential and often investigated separation [2,53–55] that shows significant similarity to isopropanol dehydration. It is of great importance in the production of bioethanol, which, in combination with biodiesel, accounts for 90% of the applied biofuels [56] and for which the global production is expected to reach about 145 billion liters by 2023 [57]. The mixture forms a minimum-boiling azeotrope at 89.1 mol% ethanol with a boiling point of 78.17 °C at atmospheric pressure [58]. The non-ideality of the liquid phase is accurately modeled with the non-random two-liquid (NRTL) model, while the vapor phase is assumed as ideal. The pure component parameters are taken from the DB-PURE32 database and the binary interaction parameters are taken from the APV88 VLE-IG and APV88 LLE-ASPEN database in Aspen Plus®, respectively. The parameter sets for the additional solvents considered in the following are also collected from these databases.

3.1.1. Solvent Selection

The proposed method's first application aims to identify a suitable solvent from a set of solvent candidates. For that purpose, separating a diluted ethanol-water fermentation broth is considered with an initial feed composition of 6 mol% ethanol [2]. An already pre-heated feed stream with a flow rate of 10 mol· s^{-1} (~709.1 kg· h^{-1}) is to be separated into product streams with a purity of at least 99.9 mol%. Four solvent candidates are selected

based on a literature review and the similarity of the mixture topology. Cyclohexane (CHEX) is chosen as the established benchmark solvent for this separation, which has effectively substituted the potentially carcinogenic benzene [6,59]. Furthermore, hexane (HEX), isooctane (ISOOCT), and toluene (TOL) are selected based on the similarity of the mixture topology, which refers to case (a) in Figure 2. The individual columns are modeled at isobaric conditions and atmospheric pressure. The initial number of stages for the simple column is set to 60 for CHEX, 70 for HEX, and 50 for ISOOCT and TOL. For the heterogeneous column, the initial number of stages was defined as 70 for CHEX, HEX, and ISOOCT, as well as 80 for TOL. For all solvent candidates, the cost of a pure make-up stream is assumed to be 1000 € $\cdot$ t^{-1}. However, a more accurate cost estimate is not necessary since the general costs of the make-up stream are negligible due to the high product purities. For all considered solvents, the make-up costs are smaller than 0.4% of the TAC of the optimized processes. The results of the solvent screening are summarized in Figure 4, which provides the costs of the individually optimized process configurations for the different solvents divided into CAPEX and OPEX. The resulting costs for CHEX and HEX are not differentiable within the expected accuracy range of the cost estimates for the conceptual design. However, the increase of the TAC for ISOOCT and TOL is more than 15% compared to CHEX with higher OPEX and CAPEX.

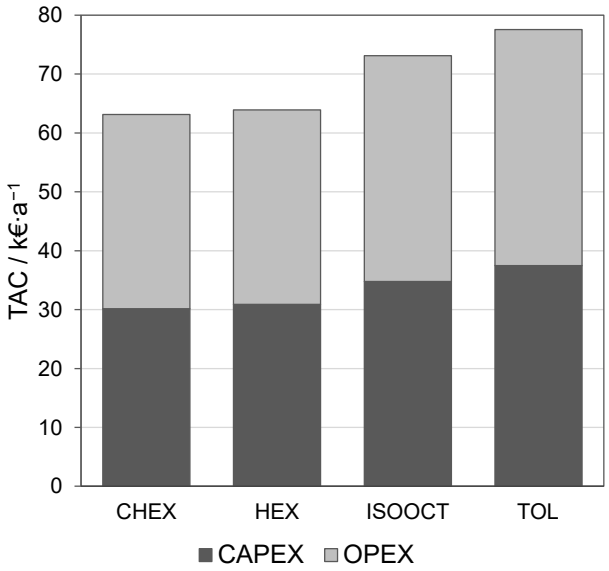

Figure 4. Total annualized costs (TAC) for the solvents cyclohexane (CHEX), hexane (HEX), isooctane (ISOOCT) and toluene (TOL) separated in capital expenditures (CAPEX) and operational expenditures (OPEX).

Figure 5 (left) shows the detailed results of the optimization-based design for the solvent CHEX, which is chosen for further investigations. The superstructure optimization effectively reduces the number of equilibrium stages of both columns, whereas the simple distillation column is slightly higher than the heteroazeotropic distillation column. The simple distillation column further requires the majority of the overall energy demand with a reboiler heat duty of 137.6 kW compared to 48.8 kW in the heteroazeotropic distillation column. While the solvent make-up stream is determined at only 4.6 $\times$ 10^{-5} mol $\cdot$ s^{-1}, it is interesting to note that the overall amount of CHEX in the system is very low. The recycle stream from the decanter is only about 6% of the feed stream and contains only 6 mol% CHEX. This is very similar to the almost equivalently performing HEX.

The Gibbs diagram with the respective initial and final liquid composition profiles of the individual columns is illustrated in Figure 5 (right). The partial linear initial profile for the heterogeneous column is simple but convenient compared to the final composition profile. Although the constant initial composition profile for the simple column is highly

shifted towards water due to the diluted feed composition, it provides sufficient starting values for the polylithic solution procedure.

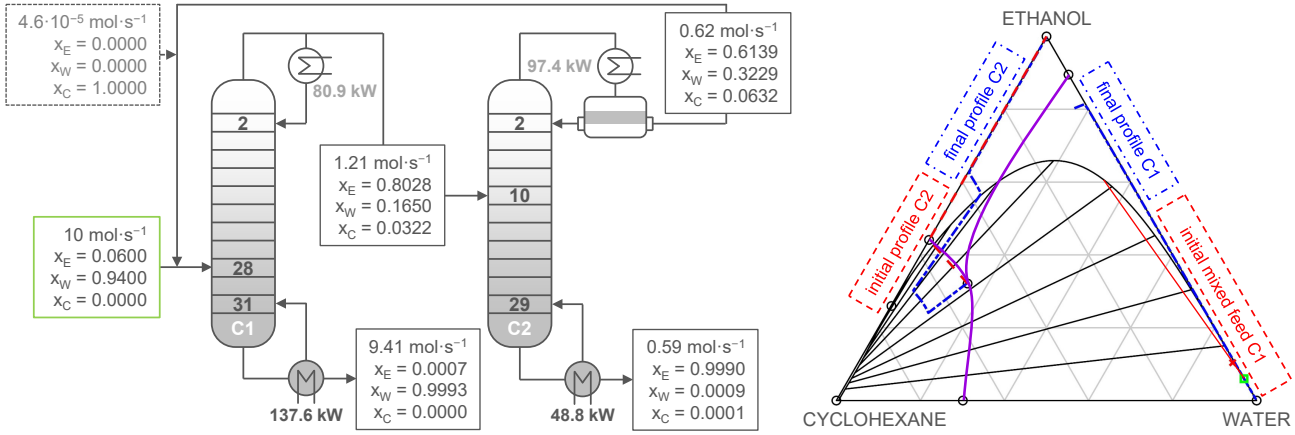

Figure 5. Optimal process design for the separation of ethanol and water using cyclohexane as a solvent in a two-column heteroazeotropic distillation setup (**left**), including the initial and final liquid composition profiles of both columns in the corresponding Gibbs diagram (**right**). The initial composition profiles of columns C1 and C2 are plotted as red cross and dashed line, respectively, while the final composition profiles of both columns are plotted as blue dot-dashed lines. The feed composition is indicated by a green square and all singular points as well as the liquid-liquid critical point are marked as black circles.

The topology-based initialization procedure allows for an effective comparison of the alternative solvents with individually optimized process designs for each solvent candidate. The computational load for the individual optimization studies is less than 10 min, such that the assessment of even larger candidate sets is feasible. Furthermore, the computational load can be effectively reduced using a multi-threading approach since the individual process optimization problems are independent and can be run in parallel.

3.1.2. Multi-Objective Optimization

A MOO problem is defined for the CHEX solvent to further analyze the optimal process design, considering CAPEX and OPEX as individual objective functions, as described in Section 2.3. Figure 6 shows the resulting set of optimal solutions indicating a convex Pareto front. These results allow for an approximation of a feasible and infeasible region for this separation task w.r.t. the predefined product constraints in the design space. Furthermore, the results indicate the structural flexibility for different variants with similar overall TAC or the respective costs for a shift in CAPEX and OPEX, which provides added information for the process engineering team during the conceptual design phase. The lowest TAC are indicated by the triangle, which corresponds to a very similar design as described previously (cf. Figure 5). The two bold lines indicate constant TAC with a deviation of +5%. Interestingly, almost all Pareto-optimal solutions lie within this 5%-interval, indicating that the process engineer has a lot of flexibility in choosing between larger equipment and higher investment or lower energy requirements and operating costs. The possible shift between CAPEX and OPEX in that range adds up to about 20% of the individual CAPEX or OPEX.

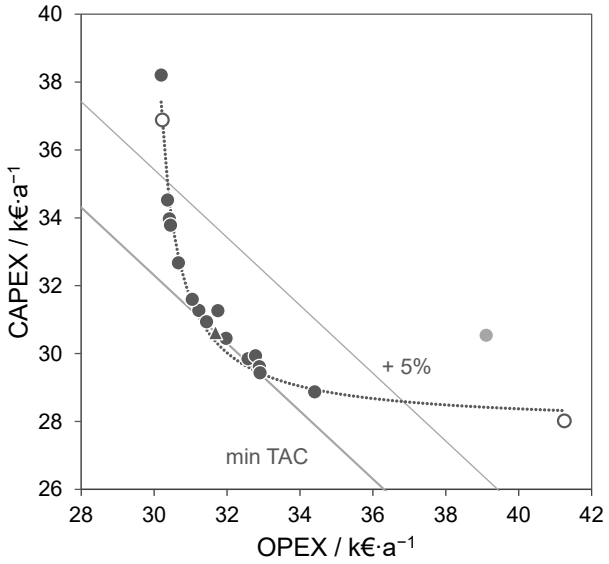

Figure 6. Set of solutions close to Pareto-optimality for the heteroazeotropic distillation of ethanol and water using cyclohexane as solvent. The white circles indicate the individual optimization of the OPEX and CAPEX, respectively, and the thick and thin lines are lines of constant TAC for the lowest costs and an additional 5%. The light-gray circle denotes a locally optimized but finally sub-optimal solution, which is not in close vicinity to the approximated Pareto front and omitted for the fit of Equation (2) shown as dotted line.

Based on the set of solutions, an approximation of the Pareto front was determined by nonlinear regression, following the model

$$\text{CAPEX} = \frac{a}{\text{OPEX} + b} + c. \tag{2}$$

One solution, obtained in the course of the optimization, is marked in light-gray, lies further in the feasible region and is treated as an outlier, although the solver status identifies it as a locally optimal solution. The solution is characterized by a decisive increase of the CAPEX, which results from the final steps of the SR-MINLP optimization in which the initially relaxed binary decision variables are forced to discrete values. It is important to note that this problem can be overcome by slight modifications of the initial feed location or the total number of stages. By omitting this data point, the resulting approximation of the Pareto front is astonishingly accurate with a coefficient of determination of $R^2 = 0.9778$. This correlation can further be used for a simple assessment of the distribution between CAPEX and OPEX. The whole set of solutions was determined in 30 min of wall-clock time in parallel runs managed by a simple Python script. While the proposed initialization procedure requires a substantial share of the overall computational time required for an individual optimization, the initialization has to be performed only once for all variations of the objective function.

3.1.3. Sensitivity Analysis

Finally, the proposed approach is applied for the evaluation of a parametric variation of the design problem, considering the application of the heteroazeotropic distillation process for varying feed compositions. The resulting sensitivity analysis provides important insight into the applicability of the process concept for different feed compositions, analyzing the flexibility as well as potential inefficiencies for varying feed conditions. The results of a wide-range variation of the feed composition are summarized in Figure 7. Note that the feed flow rate is kept constant for all cases and that the individual feed streams are assumed to be pre-heated to the individual boiling point prior to entering the process.

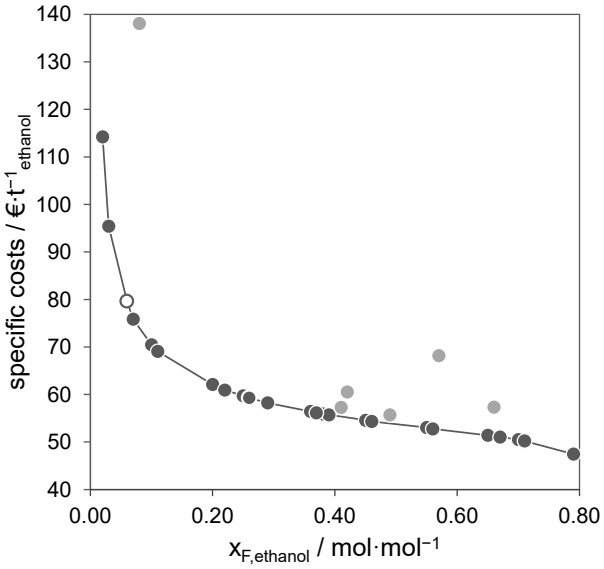

Figure 7. Specific costs of ethanol for variable feed compositions. The white circle indicates the feed composition from Sections 3.1.1 and 3.1.2.

The results show the expected trend for an increasing ethanol composition in the feed with steadily dropping specific costs. While this is qualitatively expected, since the amount of ethanol is increasing due to the fixed feed flow rate, the specific trajectory of the curve for the specific costs is of particular interest. For small ethanol compositions in the feed stream, the relative costs are decreasing rapidly from 115 $€ \cdot t^{-1}$ to roughly 60 $€ \cdot t^{-1}$ at a feed composition of up to 20 mol% followed by a substantially flatter decrease to 47 $€ \cdot t^{-1}$ close to the azeotropic composition. Consequently, a potential pre-concentration step in the range of about 20 mol% could be of interest to improve the energy and cost-efficiency of the process. This option is in line with the recommendations proposed by Blahušiak et al. [60]. Waltermann et al. [27] also investigated the potential of a pre-concentration for the dehydration of ethanol by extractive distillation and heteroazeotropic distillation but they concluded that the savings for the heteroazeotropic distillation process were too small compared to the cost for an additional distillation column. Alternatively, the effective application of a membrane-based pre-concentration was demonstrated for the purification of γ-valerolactone by an extraction-based process with thermal regeneration of the solvent in a recent study by Scharzec et al. [61].

For this case study, six outliers (light-gray circles) w.r.t. the trend of the overall specific costs result as sub-optimal solutions from the final SR-MINLP optimization. These data points could be analyzed manually by varying the structural input variables of the optimization model. In order to illustrate that the final fixation of the relaxed binary variables in the SR-MINLP is the cause of the problem for these solutions, a comparison between intermediate and final results of the solution strategy is depicted in the appendix in Figure A1. For mole fractions of ethanol below 40%, the intermediate and final data are in excellent accordance, which illustrates the correct working topology-based initialization along with the structural optimization. For higher ethanol fractions, the intermediate results for the minimum energy designs show some outliers. However, the overall trend of the majority of the intermediate data points follows a linear regression. For most of the outliers in the final cost optimization (light-gray circles), a profound initial minimum reboiler duty was calculated and provided as starting value, which shows the correct working of the topology-based initialization procedure. Similar to the previous evaluations, the sensitivity study is efficiently performed based on the proposed initialization and optimization approach. The results of the sensitivity analysis provide an increased understanding of the process performance and can aid in the identification of further improvement options. Besides the feed composition and product specifications, variations in the utility costs or depreciation times, as well as variations of the thermodynamic property data, may be evaluated.

3.2. Ethyl Acetate-Isooctane Separation

The second case study deals with the separation of ethyl acetate and isooctane, which has been investigated as a waste stream in the pharmaceutical industry [62]. The mixture exhibits a minimum-boiling azeotrope under atmospheric pressure at about 84.4 mol% of ethyl acetate and 76.3 °C [63]. Ooms et al. [62] investigated the separation of this mixture with a feed composition of 62.9 mol% ethyl acetate using heteroazeotropic batch distillation. Based on a list of 60 potential solvents, acetonitrile and methanol were selected as promising candidates, whereas acetonitrile was finally chosen as the only suitable solvent based on the mixture topology, which represents type (b) in Figure 2. Following this selection, a feed stream of 10 mol $\cdot$ s^{-1} (~3520.7 kg $\cdot$ h^{-1}) is considered with product purities of at least 99.8 mol%. The initial column setup comprises 50 stages for the simple column and 130 stages for the heteroazeotropic column. The non-ideality of the liquid phase is again described by the NRTL model with binary interaction parameters taken from the NISTV88 NIST-IG database in Aspen Plus®. Pure component parameters are taken from the DB-PURE32 database in Aspen Plus® and an ideal gas phase is assumed since all calculations are performed at atmospheric pressure.

The result of the individual process optimization is illustrated in Figure 8. Similar to the previous case study, the number of trays inside each column was reduced during the optimization, although the number of trays in the heterogeneous column is about five times greater than for the simple column. Additionally, the reboiler duty of the heterogeneous column is roughly 2.5 times greater, with a value of 1327.4 kW. The estimations of the initial composition profiles of both columns serve as excellent starting points and make the model robust and efficient.

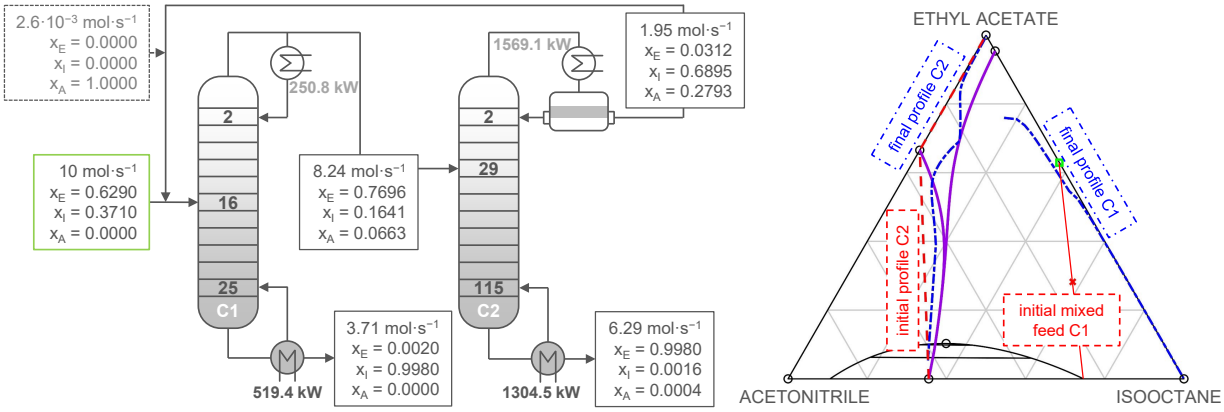

Figure 8. Optimal process design for the separation of ethyl acetate and isooctane using water as a solvent in a two-column heteroazeotropic distillation setup (**left**), including the initial and final liquid composition profiles of both columns in the corresponding Gibbs diagram (**right**). The initial composition profiles of columns C1 and C2 are plotted as red cross and dashed line, respectively, while the final composition profiles of both columns are plotted as blue dot-dashed lines. The feed composition is indicated by a green square and all singular points as well as the liquid-liquid critical point are marked as black circles.

3.2.1. Multi-Objective Optimization

The resulting approximation of the Pareto front is illustrated in Figure 9 considering CAPEX and OPEX as competing objectives. Even though the individual values for CAPEX and OPEX are significantly higher compared to the previous case study, the convex shape of the Pareto front is very similar. As for the first case study, the feasible and infeasible region can be clearly separated and a simple correlation according to Equation (2) can approximate the Pareto front with high accuracy ($R^2 = 0.9817$). Considering the range of the minimum TAC up to +5%, there is again flexibility in the cost distribution of around 20% for the CAPEX, which reflects significant differences in the structural and operational process design degrees of freedom. Interestingly, one Pareto-optimal design within this

interval corresponds to the nadir point for the CAPEX. This behavior is induced by the difference in magnitude of the two objective functions and can be traced back to the predefined depreciation time and interest rate. Fortunately, the automated characteristics of the presented calculation allow the investigation of different Pareto-optimal sets of solutions by adjusting the depreciation time and the interest rate.

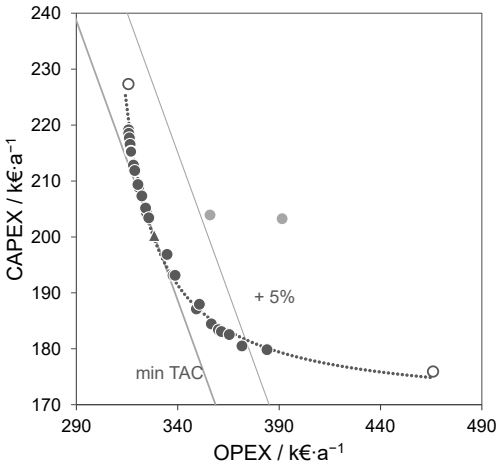

Figure 9. Set of Pareto-optimal solutions for the heteroazeotropic distillation of ethyl acetate and isooctane using acetonitrile as solvent. The white circles indicate the individual optimization of the OPEX and CAPEX, respectively, and the thick and thin lines are lines of constant TAC for the lowest costs and an additional 5%. The light-gray circles denote locally optimized but finally sub-optimal solutions, which are not in close vicinity to the approximated Pareto front and omitted for the fit of Equation (2) shown as a dotted line.

3.2.2. Sensitivity Analysis

Figure 10 illustrates the results of the sensitivity analysis for a variable feed composition. The behavior is similar to that shown for the ethanol-water mixture. For low concentrated feed streams, the specific costs are comparably high and decrease rapidly, reaching almost a plateau at 35–40 € · t^{-1}. Since the initially considered feed composition (white circle) is significantly higher than for the previous ethanol-water separation, a preconcentration would, in this case, not be reasonable since the actual feed composition is already located in the region of "low-specific cost".

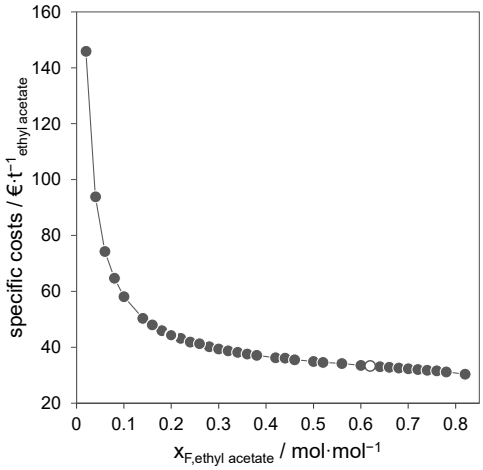

Figure 10. Specific costs of ethyl acetate for variable feed compositions. The white circle indicates the feed composition from Section 3.2.1.

The calculations presented here are carried out over the whole composition space below the azeotropic concentration of ethyl acetate. Due to significant variations in the required number of stages, it is not recommended to use a single initialization determined for one of the potential feed compositions. Rather, the initialization is adjusted in case of larger variations for different intervals of the feed compositions. A similar approach is recommended in case of variations of other parameters than the feed flow rate.

3.3. 1,4-Dioxane Dehydration

The third and last case study considers the dehydration of 1,4-dioxane, which is frequently applied as a solvent in the pharmaceutical and petrochemical industry [64]. The mixture of 1,4-dioxane and water forms a minimum-boiling azeotrope at around 47.2 mol% 1,4-dioxane and 87.5 °C [65]. With a boiling point of about 101 °C, 1,4-dioxane and water are particularly close-boiling [66], such that the mixture is considered extremely hard to separate by means of distillation. For higher concentrations of 1,4-dioxane close to and above the azeotropic composition, Kuila and Ray [64] as well as Singha et al. [66] suggest a separation using pervaporation. For lower concentrated mixtures, including triethylamine impurities, Wu et al. [67] suggest a separation by heteroazeotropic distillation and compared this to pressure-swing distillation. Considering further intensification in terms of a dividing wall column for the heteroazeotropic distillation process, they report significant savings in TAC (~43%) compared to the pressure-swing distillation process. Skouras and Skogestad [37] also investigated the dehydration of 1,4-dioxane with benzene as a solvent in a batch heteroazeotropic distillation process. The ternary system with benzene is an example for the topology (c) in Figure 2 and it is further evaluated with a moderately concentrated feed with a mole fraction of 30 mol% of 1,4-dioxane in water and a flow rate of 10 mol $\cdot$ s^{-1} (~1405.5 kg $\cdot$ h^{-1}). The purity constraints for the product streams of 1,4-dioxane and water are set to 99.8 mol%. The initial number of stages is set to 50 for the simple column and 60 for the heteroazeotropic column. The non-ideality of the liquid phase is again described by the NRTL model in combination with an ideal gas phase. The columns are operated at atmospheric pressure. The pure component parameters are taken from the DB-PURE38 database and the binary interaction parameters are taken from the APV120 VLE-IG and APV120 LLE-ASPEN database in Aspen Plus®, respectively.

The detailed results of the process optimization are illustrated in Figure 11. In both columns, the number of trays is reduced successfully, with the simple column being about double the size of the heteroazeotropic column. Interestingly, the first column is entirely reduced to a stripping column, while the rectifying section in the heterogeneous column is also almost omitted completely. Feeding the distillate vapor stream without condensation to the heteroazeotropic column saves about 59% of the energy in the reboiler resulting in a duty of 163.3 kW in contrast to 401.5 kW. As opposed to the previous case studies, the optimization procedure relies on a small purge stream, which is optional for all considered case studies. One explanation for this slightly reduced robustness could be the inferior estimation of the initial composition profile of the heteroazeotropic column. Nevertheless, the purge stream accounts for only 0.8% of the feed stream and can be tolerated.

3.3.1. Multi-Objective Optimization

The resulting approximation of the Pareto front is illustrated in Figure 12. While the individual objectives (white circles) are more pronounced extremes that deviate further from the indicated 5% interval, most of the determined solutions fall within the interval indicating the flexibility in the cost distribution. The flat optimum around the lowest TAC is especially noticeable for this case study with several individual designs with almost equivalent TAC values. Thus, the MOO approach also provides an effective tool to explore the distinctness of the individual optimal solution determined from the SOO. The data allow for a proper regression with a coefficient of determination of $R^2 = 0.9607$. As for the previous cases, a few outliers are not considered during the regression of Equation (2). In Figure 12, only one outlier is represented (light-gray circle) since the focus is given to

the data points close to the Pareto front, while a complete depiction of the obtained results is presented in the appendix in Figure A2. There are five solutions with an increase of 24–41% in the TAC compared to the best found process design, which is caused by the previously described problems in the final steps of the SR-MINLP optimization, fixing the binary decision variables. However, these optimization runs could still be investigated by altering the input data, as mentioned in Section 3.1.2.

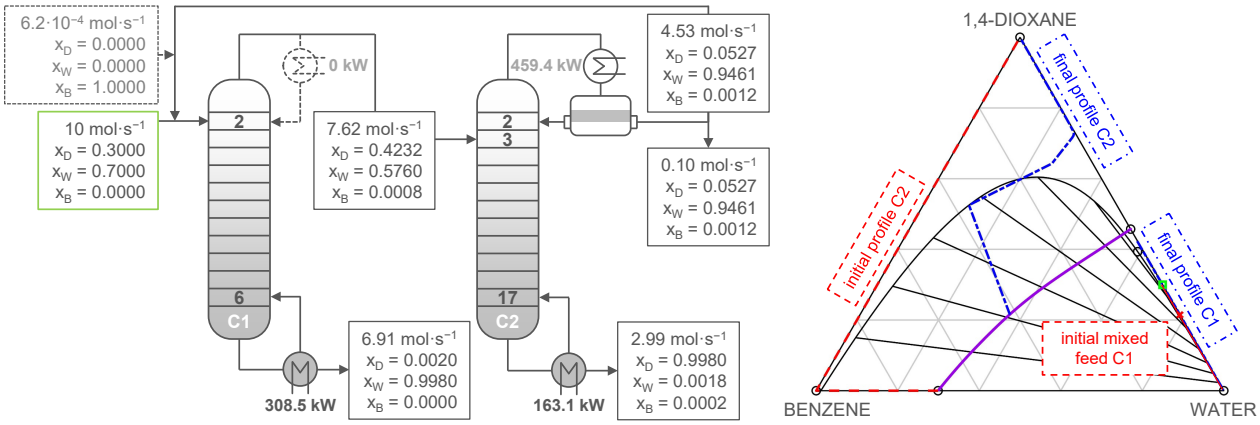

Figure 11. Optimal process design for the separation of 1,4-dioxane and water using benzene as a solvent in a two-column heteroazeotropic distillation setup (**left**), including the initial and final liquid composition profiles of both columns in the corresponding Gibbs diagram (**right**). The initial composition profiles of columns C1 and C2 are plotted as red cross and dashed line, respectively, while the final composition profiles of both columns are plotted as blue dot-dashed lines. The feed composition is indicated by a green square and all singular points as well as the liquid-liquid critical point are marked as black circles.

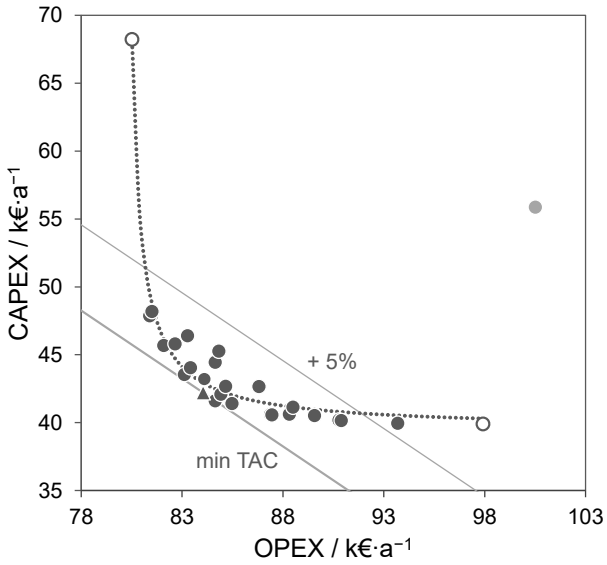

Figure 12. Set of solutions close to Pareto-optimality for the heteroazeotropic distillation of 1,4-dioxane and water using benzene as solvent. The white circles indicate the individual optimization of the OPEX and CAPEX, respectively, and the thick and thin lines are lines of constant TAC for the lowest costs and an additional 5%. The light-gray circle denotes a locally optimized but finally sub-optimal solution, which is not in close vicinity to the approximated Pareto front and omitted for the fit of Equation (2) shown as a dotted line.

3.3.2. Sensitivity Analysis

Figure 13 illustrates the results of the sensitivity analysis for a variable feed composition in the range of low to azeotropic compositions. Interestingly, the relationship between the specific costs and the 1,4-dioxane composition of the feed stream is more linear compared to the previous two examples, indicating the potential benefit of a pre-concentration step, as discussed for the ethanol-water example in Section 3.1.3. Furthermore, this behavior highlights the importance of a case-specific evaluation since the case studies do not indicate a possible simple generalization in terms of heuristic rules.

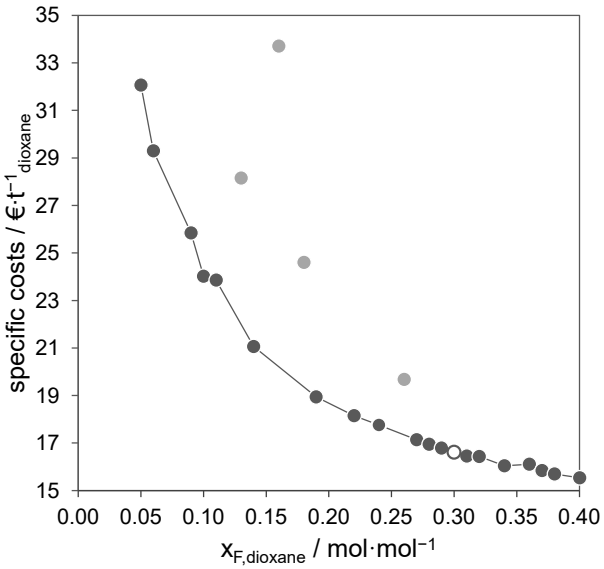

Figure 13. Specific costs of 1,4-dioxane for variable feed compositions. The white circle indicates the feed composition from Section 3.3.1.

In contrast to the other case studies, there is a slightly reduced convergence rate for low 1,4-dioxane fractions as well as four sub-optimal results, which clearly deviate from the overall progression of the other solutions (light-gray circles). However, the intermediate results during the polylithic solution procedure for a design with a minimum energy demand, depicted in the appendix in Figure A3, indicate the excellent topology-based initialization since most of the results follow the clear trend (blue line). Two exceptions lead to non-optimal results when the recycle stream is closed (light blue triangles). The results also show that the introduction of the cost and sizing equations, as well as the solution of the relaxed MINLP problems, tremendously increase the complexity of the model. Nonetheless, the overall performance along with the gained results emphasize the advantages of the presented topology-based initialization strategy.

4. Discussion

Heteroazeotropic distillation processes present an interesting hybrid process for energy and cost-efficient separation of azeotropic mixtures in industry. Yet, there are far fewer studies investigating these process concepts compared to pressure-swing and extractive distillation. The complexity associated with the simulation and optimization of these hybrid processes, which require the correct solution of the vapor-(liquid)-liquid equilibrium relationship, is presumably one of the reasons that impede a more widespread consideration. The proposed topology-based initialization and optimization approach enables a numerically efficient and reliable optimization of heteroazeotropic distillation processes without needing an initial feasible process simulation. This allows for an automatic evaluation of commonly time-consuming tasks, including solvent screening, sensitivity analysis, and multi-objective optimization studies. The applicability of the approach is demonstrated

for the separation of three practically relevant azeotropic mixtures, which in combination with the considered solvents, cover the three most common ternary mixture topologies for solvent-induced heteroazeotropic distillation.

The results of the single and multi-objective optimization studies and the sensitivity studies illustrate the added value of such an optimization-based design approach. On the one hand, different solvent candidates can be evaluated and compared based on the individually optimized processes. On the other hand, parametric variations can effectively assess the sensitivity and flexibility of the individual designs. This allows for the analysis of potential variation that the process engineers can exploit during the conceptual design or the identification of possible improvements, such as the discussed pre-concentration for more efficient utilization of the heteroazeotropic distillation process.

The latter will be investigated in future work, building on the motivating results for an extraction-based separation process [61]. Furthermore, the evaluation of different means for energy integration [50] will be evaluated in combination with the sensitivity studies to compare various process alternatives comprehensively. The reported results demonstrate the reliability and improved performance of the proposed initialization and optimization approach. However, the automated results also revealed the occasional occurrence of sub-optimal solutions, which was traced back to problems in the final steps of the SR-MINLP approach when fixing the binary decision variables. The investigations will also be extended to handle mixtures with more components and special topologies, e.g., open miscibility gaps.

Author Contributions: Conceptualization, K.F.K. and M.S.; methodology, K.F.K. and M.S.; software, K.F.K. and M.S.; validation, K.F.K.; formal analysis, K.F.K.; investigation, K.F.K. and M.S.; data curation, K.F.K.; writing—original draft preparation, K.F.K.; writing—review and editing, K.F.K. and M.S.; visualization, K.F.K.; supervision, M.S.; funding, M.S. All authors have read and agreed to the published version of the manuscript.

Funding: Publishing fees funded by the Deutsche Forschungsgemeinschaft (DFG, German Research Foundation)-Projektnummer 491268466 and the Hamburg University of Technology (TUHH) in the funding program "Open Access Publishing".

Institutional Review Board Statement: Not applicable.

Informed Consent Statement: Not applicable.

Conflicts of Interest: The authors declare no conflict of interest.

Abbreviations

The following abbreviations are used in this manuscript:

CAMD	Computer-Aided Molecular Design
CAPEX	Capital Expenditures
CHEX	Cyclohexane
GAMS	General Algebraic Modeling System
HEX	Hexane
ISOOCT	Isooctane
MESH	Mass, Equilibrium, Summation, and Enthalpy
MINLP	Mixed-Integer Nonlinear Programming
MOO	Multi-Objective Optimization
NCP	Nonlinear Complementary Constraint
NLP	Nonlinear Programming
OPEX	Operational Expenditures
SOO	Single Objective Optimization
SR-MINLP	Successively Relaxed Mixed-Integer Nonlinear Programming
TAC	Total Annualized Costs
TOL	Toluene
VLE	Vapor-Liquid Equilibrium
VLLE	Vapor-Liquid-Liquid Equilibrium

Appendix A

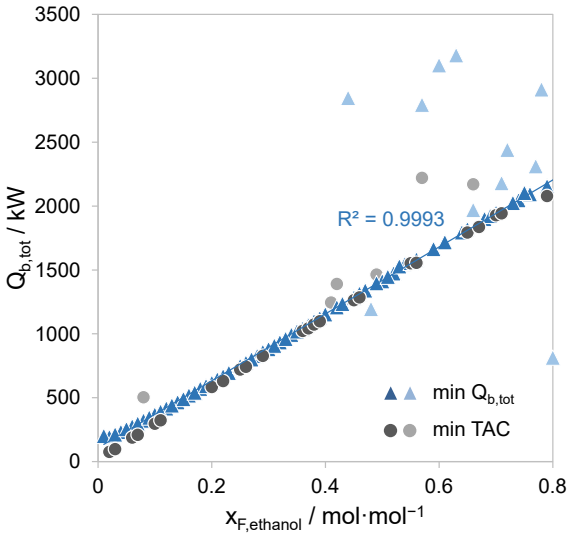

Figure A1. Set of solutions for the heteroazeotropic distillation of ethanol and water using cyclohexane as solvent. The blue triangles represent intermediate results during the polylithic solution strategy without cost and sizing equations, considering the total reboiler duty as the objective function. The circles mark the final results after the structural optimization w.r.t. the total annualized costs (TAC). The light-gray circles correspond to the outliers in Figure 7.

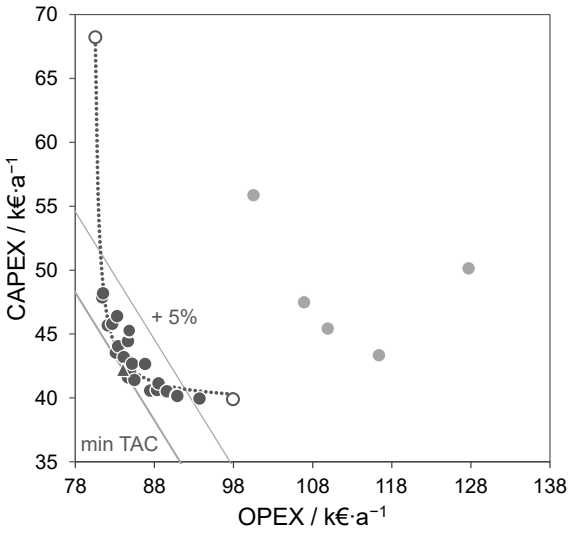

Figure A2. Set of solutions close to Pareto-optimality for the heteroazeotropic distillation of 1,4-dioxane and water using benzene as solvent. The white circles indicate the individual optimization of the OPEX and CAPEX, respectively, and the thick and thin lines are lines of constant TAC for the lowest costs and an additional 5%. The light-gray circles denote local optimal solutions, which are not in close vicinity to the approximated Pareto front and omitted for the fit of Equation (2) shown as a dotted line.

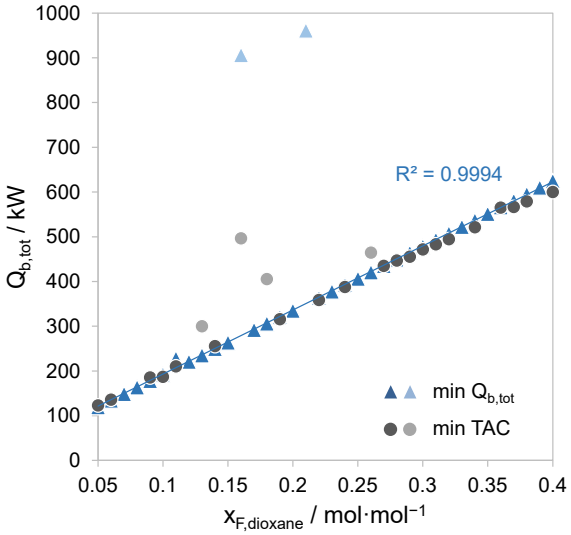

Figure A3. Set of solutions for the heteroazeotropic distillation of 1,4-dioxane and water using benzene as solvent. The blue triangles represent intermediate results during the polylithic solution strategy without cost and sizing equations, considering the total reboiler duty as the objective function. The circles mark the final results after the structural optimization w.r.t. the total annualized costs (TAC). The light-gray circles correspond to the outliers in Figure 13.

References

1. Gerbaud, V.; Rodriguez-Donis, I.; Hegely, L.; Lang, P.; Denes, F.; You, X. Review of extractive distillation. Process design, operation, optimization and control. *Chem. Eng. Res. Des.* **2019**, *141*, 229–271. [CrossRef]
2. Kiss, A.A.; Suszwalak, D.J.P. Enhanced bioethanol dehydration by extractive and azeotropic distillation in dividing-wall columns. *Sep. Purif. Technol.* **2012**, *86*, 70–78. [CrossRef]
3. Skiborowski, M.; Harwardt, A.; Marquardt, W. Conceptual design of distillation-based hybrid separation processes. *Annu. Rev. Chem. Biomol. Eng.* **2013**, *4*, 45–68. [CrossRef]
4. Kiva, V.N.; Hilmen, E.K.; Skogestad, S. Azeotropic phase equilibrium diagrams: A survey. *Chem. Eng. Sci.* **2003**, *58*, 1903–1953. [CrossRef]
5. Skiborowski, M.; Bausa, J.; Marquardt, W. A Unifying Approach for the Calculation of Azeotropes and Pinch Points in Homogeneous and Heterogeneous Mixtures. *Ind. Eng. Chem. Res.* **2016**, *55*, 6815–6834. [CrossRef]
6. Furzer, I.A. Synthesis of entrainers in heteroazeotropic distillation systems. *Can. J. Chem. Eng.* **1994**, *72*, 358–364. [CrossRef]
7. Gani, R.; Nielsen, B.; Fredenslund, A. A group contribution approach to computer-aided molecular design. *AIChE J.* **1991**, *37*, 1318–1332. [CrossRef]
8. Doherty, M.F.; Malone, M.F. *Conceptual Design of Distillation Systems*, 1st ed.; McGraw-Hill Chemical Engineering Series; McGraw-Hill: Boston, MA, USA, 2001.
9. Gmehling, J.; Schedemann, A. Selection of Solvents or Solvent Mixtures for Liquid–Liquid Extraction Using Predictive Thermodynamic Models or Access to the Dortmund Data Bank. *Ind. Eng. Chem. Res.* **2014**, *53*, 17794–17805. [CrossRef]
10. Zhou, T.; Song, Z.; Zhang, X.; Gani, R.; Sundmacher, K. Optimal Solvent Design for Extractive Distillation Processes: A Multiobjective Optimization-Based Hierarchical Framework. *Ind. Eng. Chem. Res.* **2019**, *58*, 5777–5786. [CrossRef]
11. Luyben, W.L. *Distillation Design and Control Using Aspen Simulation*, 2nd ed.; Elektronische Ressource ed.; Wiley and AIChE: Hoboken, NJ, USA; New York, NY, USA, 2013. [CrossRef]
12. Huang, X.; Li, Z.; Tian, Y. Process optimization of an industrial acetic acid dehydration progress via heterogeneous azeotropic distillation. *Chin. J. Chem. Eng.* **2018**, *26*, 1631–1643. [CrossRef]
13. Vazquez-Castillo, J.A.; Venegas-Sánchez, J.A.; Segovia-Hernández, J.G.; Hernández-Escoto, H.; Hernández, S.; Gutiérrez-Antonio, C.; Briones-Ramírez, A. Design and optimization, using genetic algorithms, of intensified distillation systems for a class of quaternary mixtures. *Comput. Chem. Eng.* **2009**, *33*, 1841–1850. [CrossRef]
14. Yang, X.L.; Ward, J.D. Extractive Distillation Optimization Using Simulated Annealing and a Process Simulation Automation Server. *Ind. Eng. Chem. Res.* **2018**, *57*, 11050–11060. [CrossRef]
15. Li, X.; Cui, C.; Li, H.; Gao, X. Process synthesis and simulation-based optimization of ethylbenzene/styrene separation using double-effect heat integration and self-heat recuperation technology: A techno-economic analysis. *Sep. Purif. Technol.* **2019**, *228*, 115760. [CrossRef]
16. Ramanathan, S.P.; Mukherjee, S.; Dahule, R.K.; Ghosh, S.; Rahman, I.; Tambe, S.S.; Ravetkar, D.D.; Kulkarni, B.D. Optimization of Continuous Distillation Columns Using Stochastic Optimization Approaches. *Chem. Eng. Res. Des.* **2001**, *79*, 310–322. [CrossRef]

17. Brüggemann, S.; Oldenburg, J.; Zhang, P.; Marquardt, W. Robust Dynamic Simulation of Three-Phase Reactive Batch Distillation Columns. *Ind. Eng. Chem. Res.* **2004**, *43*, 3672–3684. [CrossRef]
18. Skiborowski, M.; Harwardt, A.; Marquardt, W. Efficient optimization-based design for the separation of heterogeneous azeotropic mixtures. *Comput. Chem. Eng.* **2015**, *72*, 34–51. [CrossRef]
19. Franke, M.B. MINLP optimization of a heterogeneous azeotropic distillation process: Separation of ethanol and water with cyclohexane as an entrainer. *Comput. Chem. Eng.* **2016**, *89*, 204–221. [CrossRef]
20. Luyben, W.L. Control of a multiunit heterogeneous azeotropic distillation process. *AIChE J.* **2006**, *52*, 623–637. [CrossRef]
21. Kong, Z.Y.; Lee, H.Y.; Sunarso, J. The evolution of process design and control for ternary azeotropic separation: Recent advances in distillation and future directions. *Sep. Purif. Technol.* **2022**, *284*, 120292. [CrossRef]
22. Guang, C.; Shi, X.; Zhang, Z.; Wang, C.; Wang, C.; Gao, J. Comparison of heterogeneous azeotropic and pressure-swing distillations for separating the diisopropylether/isopropanol/water mixtures. *Chem. Eng. Res. Des.* **2019**, *143*, 249–260. [CrossRef]
23. Guang, C.; Shi, X.; Zhao, X.; Zhang, Z.; Li, G. Development and intensification of a four-column hybrid process of heteroazeotropic distillation and pressure-swing distillation. *Chem. Eng. Process. Process. Intensif.* **2020**, *150*, 107875. [CrossRef]
24. Guang, C.; Zhao, X.; Zhang, Z.; Gao, J.; Li, M. Optimal design and performance enhancement of heteroazeotropic and pressure-swing coupling distillation for downstream isopropanol separation. *Sep. Purif. Technol.* **2020**, *242*, 116836. [CrossRef]
25. Bausa, J.; Marquardt, W. Quick and reliable phase stability test in VLLE flash calculations by homotopy continuation. *Comput. Chem. Eng.* **2000**, *24*, 2447–2456. [CrossRef]
26. Kraemer, K.; Harwardt, A.; Skiborowski, M.; Mitra, S.; Marquardt, W. Shortcut-based design of multicomponent heteroazeotropic distillation. *Chem. Eng. Res. Des.* **2011**, *89*, 1168–1189. [CrossRef]
27. Waltermann, T.; Grueters, T.; Muenchrath, D.; Skiborowski, M. Efficient optimization-based design of energy-integrated azeotropic distillation processes. *Comput. Chem. Eng.* **2020**, *133*, 106676. [CrossRef]
28. Kraemer, K.; Kossack, S.; Marquardt, W. Efficient Optimization-Based Design of Distillation Processes for Homogeneous Azeotropic Mixtures. *Ind. Eng. Chem. Res.* **2009**, *48*, 6749–6764. [CrossRef]
29. Aachener Verfahrenstechnik. Process Synthesis Software Collection. Available online: https://www.avt.rwth-aachen.de/cms/AVT/Forschung/Software/~iptu/Softwaresammlung-Prozesssynthese (accessed on 27 July 2022).
30. Brusis, D. *Synthesis and Optimisation of Distillation Processes with MINLP Techniques*; Fortschrittberichte VDI: Reihe 3, Nr. 797, VDI Verlag: Düsseldorf, Germany, 2003.
31. Guthrie, K.M. Data and techniques for preliminary capital cost estimating. *Chem. Eng. Technol.* **1969**, *76*, 114–142.
32. Biegler, L.T.; Grossmann, I.E.; Westerberg, A.W. *Systematic Methods of Chemical Process Design*; Prentice-Hall International Series in the Physical and Chemical Engineering Sciences, Prentice-Hall: Upper Saddle River, NJ, USA, 1997.
33. Economic Indicators. Chemical Engineering Plant Cost Index. *Chem. Eng.* **2018**, *64*.
34. Rooks, R.E.; Julka, V.; Doherty, M.F.; Malone, M.F. Structure of Distillation Regions for Multicomponent Azeotropic Mixtures. *AIChE J.* **1998**, *44*, 1382–1391. [CrossRef]
35. Sasi, T.; Wesselmann, J.; Kuhlmann, H.; Skiborowski, M. Automatic synthesis of distillation processes for the separation of azeotropic multi-component systems. *Comput. Aided Chem. Eng.* **2019**, *46*, 49–54. [CrossRef]
36. Kiva, V.N.; Krolikowski, L.J. Feasibility of separation for distillation of azeotropic ternary mixtures: A survey and analysis. *Chem. Eng. Res. Des.* **2015**, *95*, 195–210. [CrossRef]
37. Skouras, S.; Skogestad, S. Separation of ternary heteroazeotropic mixtures in a closed multivessel batch distillation–decanter hybrid. *Chem. Eng. Process. Process. Intensif.* **2004**, *43*, 291–304. [CrossRef]
38. Ryll, O.; Blagov, S.; Hasse, H. ∞/∞-Analysis of heterogeneous distillation processes. *Chem. Eng. Sci.* **2013**, *104*, 374–388. [CrossRef]
39. Skiborowski, M.; Recker, S.; Marquardt, W. Shortcut-based optimization of distillation-based processes by a novel reformulation of the feed angle method. *Chem. Eng. Res. Des.* **2018**, *132*, 135–148. [CrossRef]
40. Fidkowski, Z.T.; Malone, M.F.; Doherty, M.F. Computing azeotropes in multicomponent mixtures. *Comput. Chem. Eng.* **1993**, *17*, 1141–1155. [CrossRef]
41. Bortz, M.; Burger, J.; Asprion, N.; Blagov, S.; Böttcher, R.; Nowak, U.; Scheithauer, A.; Welke, R.; Küfer, K.H.; Hasse, H. Multi-criteria optimization in chemical process design and decision support by navigation on Pareto sets. *Comput. Chem. Eng.* **2014**, *60*, 354–363. [CrossRef]
42. Marler, R.T.; Arora, J.S. Survey of multi-objective optimization methods for engineering. *Struct. Multidiscip. Optim.* **2004**, *26*, 369–395. [CrossRef]
43. Kim, I.Y.; de Weck, O.L. Adaptive weighted sum method for multiobjective optimization: A new method for Pareto front generation. *Struct. Multidiscip. Optim.* **2006**, *31*, 105–116. [CrossRef]
44. Haimes, Y.Y.; Lasdon, L.S.; Wismer, D.A. On a Bicriterion Formulation of the Problems of Integrated System Identification and System Optimization. *IEEE Trans. Syst. Man Cybern.* **1971**, *1*, 296–297. [CrossRef]
45. Das, I.; Dennis, J.E. Normal-Boundary Intersection: A New Method for Generating the Pareto Surface in Nonlinear Multicriteria Optimization Problems. *SIAM J. Optim.* **1998**, *8*, 631–657. [CrossRef]
46. Srinivas, N.; Deb, K. Muiltiobjective Optimization Using Nondominated Sorting in Genetic Algorithms. *Evol. Comput.* **1994**, *2*, 221–248. [CrossRef]

47. Deb, K.; Pratap, A.; Agarwal, S.; Meyarivan, T. A fast and elitist multiobjective genetic algorithm: NSGA-II. *IEEE Trans. Evol. Comput.* **2002**, *6*, 182–197. [CrossRef]
48. Miettinen, K. *Nonlinear Multiobjective Optimization*; International Series in Operations Research & Management Science; Springer: Boston, MA, USA, 1998; Volume 12. [CrossRef]
49. Chang, K.H. Multiobjective Optimization and Advanced Topics. In *e-Design*; Elsevier: Amsterdam, The Netherlands, 2015; pp. 1105–1173. [CrossRef]
50. Waltermann, T.; Skiborowski, M. Efficient optimization-based design of energy-integrated distillation processes. *Comput. Chem. Eng.* **2019**, *129*, 106520. [CrossRef]
51. Deb, K.; Miettinen, K.; Chaudhuri, S. Toward an Estimation of Nadir Objective Vector Using a Hybrid of Evolutionary and Local Search Approaches. *IEEE Trans. Evol. Comput.* **2010**, *14*, 821–841. [CrossRef]
52. Burger, J.; Papaioannou, V.; Gopinath, S.; Jackson, G.; Galindo, A.; Adjiman, C.S. A hierarchical method to integrated solvent and process design of physical CO_2 absorption using the SAFT-γ Mie approach. *AIChE J.* **2015**, *61*, 3249–3269. [CrossRef]
53. Roth, T.; Kreis, P.; Górak, A. Process analysis and optimisation of hybrid processes for the dehydration of ethanol. *Chem. Eng. Res. Des.* **2013**, *91*, 1171–1185. [CrossRef]
54. Klinov, A.V.; Malygin, A.V.; Khairullina, A.R.; Dulmaev, S.E.; Davletbaeva, I.M. Alcohol Dehydration by Extractive Distillation with Use of Aminoethers of Boric Acid. *Processes* **2020**, *8*, 1466. [CrossRef]
55. Kumakiri, I.; Yokota, M.; Tanaka, R.; Shimada, Y.; Kiatkittipong, W.; Lim, J.W.; Murata, M.; Yamada, M. Process Intensification in Bio-Ethanol Production–Recent Developments in Membrane Separation. *Processes* **2021**, *9*, 1028. [CrossRef]
56. Segovia-Hernández, J.G.; Sánchez-Ramírez, E. Current status and future trends of computer-aided process design, applied to purification of liquid biofuels, using process intensification: A short review. *Chem. Eng. Process. Process. Intensif.* **2022**, *172*, 108804. [CrossRef]
57. Bajpai, P. Global Production of Bioethanol. In *Developments in Bioethanol*; Bajpai, P., Ed.; Green Energy and Technology; Springer Singapore: Singapore, 2021; pp. 177–196. [CrossRef]
58. Lai, H.S.; Lin, Y.F.; Tu, C.H. Isobaric (vapor+liquid) equilibria for the ternary system of (ethanol+water+1,3-propanediol) and three constituent binary systems at P = 101.3 kPa. *J. Chem. Thermodyn.* **2014**, *68*, 13–19. [CrossRef]
59. Urdaneta, R.Y.; Bausa, J.; Brüggemann, S.; Marquardt, W. Analysis and Conceptual Design of Ternary Heterogeneous Azeotropic Distillation Processes. *Ind. Eng. Chem. Res.* **2002**, *41*, 3849–3866. [CrossRef]
60. Blahušiak, M.; Kiss, A.A.; Babic, K.; Kersten, S.R.; Bargeman, G.; Schuur, B. Insights into the selection and design of fluid separation processes. *Sep. Purif. Technol.* **2018**, *194*, 301–318. [CrossRef]
61. Scharzec, B.; Kruber, K.F.; Skiborowski, M. Model-based evaluation of a membrane-assisted hybrid extraction-distillation process for energy and cost-efficient purification of diluted aqueous streams. *Chem. Eng. Sci.* **2021**, *240*, 116650. [CrossRef]
62. Ooms, T.; Vreysen, S.; van Baelen, G.; Gerbaud, V.; Rodriguez-Donis, I. Separation of ethyl acetate–isooctane mixture by heteroazeotropic batch distillation. *Chem. Eng. Res. Des.* **2014**, *92*, 995–1004. [CrossRef]
63. Gmehling, J.; Menke, J.; Krafczyk, J.; Fischer, K. *Azeotropic Data*, 2nd ed.; Wiley-VCH: Weinheim, Germany, 2004.
64. Kuila, S.B.; Ray, S.K. Dehydration of dioxane by pervaporation using filled blend membranes of polyvinyl alcohol and sodium alginate. *Carbohydr. Polym.* **2014**, *101*, 1154–1165. [CrossRef] [PubMed]
65. Gmehling, J.; Menke, J.; Krafczyk, J.; Fischer, K.; Fontaine, J.C.; Kehiaian, H.V. Azeotropic data for binary mixtures. In *CRC Handbook of Chemistry and Physics*; CRC Press: Boca Raton, FL, USA, 2005; Volume 86.
66. Singha, N.R.; Parya, T.K.; Ray, S.K. Dehydration of 1,4-dioxane by pervaporation using filled and crosslinked polyvinyl alcohol membrane. *J. Membr. Sci.* **2009**, *340*, 35–44. [CrossRef]
67. Wu, Y.C.; Huang, H.P.; Chien, I.L. Investigation of the Energy-Saving Design of an Industrial 1,4-Dioxane Dehydration Process with Light Feed Impurity. *Ind. Eng. Chem. Res.* **2014**, *53*, 15667–15685. [CrossRef]